START

FY-1988
SST
Task 20

MORGAN, LARRY G.

RHO-LD-171
Informal Report

-201
0011786
42

DOCUMENT CONTROL

Heat Transfer Analysis for In Situ Disposal of Nuclear Wastes in Single- and Double-Shell Underground Storage Tanks

G.D. Campbell

APPROVED FOR
PUBLIC RELEASE
10/15/90 M. Dolis

REFERENCE COPY

Prepared for the United States
Department of Energy
Under Contract DE-AC06-77RL01030

NOV 1990
RECEIVED
EDMC

RECORD
COPY

RECEIVED
JUL 20 1988
L. G. MORGAN

Rockwell International

Rockwell Hanford Operations
Energy Systems Group
Richland, WA 99352

9112054058

Rockwell International
Rockwell Hanford Operations
Energy Systems Group
Richland, WA 99352

PRELIMINARY REPORT

This report contains information of a preliminary nature. It is subject to revision or correction and therefore does not represent a final report. It was prepared primarily for internal use within Rockwell Hanford Operations. Any expressed views and opinions are those of the author and not necessarily of the Company.

DISCLAIMER

This report was prepared as an account of work sponsored by an agency of the United States Government. Neither the United States Government nor any agency thereof, nor any of their employees, makes any warranty, express or implied, or assumes any legal liability or responsibility for the accuracy, completeness, or usefulness of any information, apparatus, product or process disclosed, or represents that its use would not infringe privately owned rights. Reference herein to any specific commercial product, process, or service by trade name, trademark, manufacturer, or otherwise, does not necessarily constitute or imply its endorsement, recommendation, or favoring by the United States Government or any agency thereof. The views and opinions of authors expressed herein do not necessarily state or reflect those of the United States Government or any agency thereof.

9112054050 9

INTRODUCTION

BACKGROUND

Radioactive waste resulting from reprocessing nuclear fuel is stored in underground storage (UGS) tanks at the Hanford Site. Based upon limited data on estimates of transuranic isotopes in the waste and emerging criteria for disposal of radioactive waste, it is expected that some in-tank radioactive waste will qualify for near-surface disposal in the existing waste tanks (in situ disposal). Implementation of in situ waste disposal would require drying of the damp salt cake and sludge to an acceptable level, solidification of the residual liquors and slurries, provision of support to the tank dome, and finally, installation of an earth-rock cover over each tank farm.(1)

These operations, if implemented, would affect the heat transfer characteristics of the waste storage tanks. Heat generated by fission product decay is currently transferred to the surrounding soil and to the atmosphere mainly by conduction and in some tanks by forced air ventilation. Under the in situ disposal alternative, tank ventilation would be terminated. Drying or immobilizing the waste would tend to lower its thermal conductivity. Backfilling the tank dome void spaces and building an earth cover over the tank farms would further restrict heat transfer by increasing the resistance to heat transfer between the waste and the atmosphere.

According to the radioactive waste inventory in Reference 2, the total heat loading (decayed to 1995) of all the UGS tanks is about 1.74 million Btu/hr. If evenly distributed among all 169 tanks, the average heat loading per tank would be 10,300 Btu/hr; if evenly distributed among all 75-ft-diameter single-shell tanks, the average heat loading per tank would be 13,100 Btu/hr. A list of tanks with estimated heat loadings is included in Appendix A.

This study was performed as part of the Long-Term High-Level Defense Waste Program (AR-D5-15-10).

9 1 1 2 0 5 4 0 5 1 0

PURPOSE

A parametric heat transfer analysis was conducted for predicting peak waste and concrete temperatures for long-term, in situ disposal of high-level radioactive waste. Families of maximum temperature versus total radiogenic power graphs were prepared for variable waste depths, backfill materials and tank types, and for tanks with 4 m (13.12 ft) of earth cover added to the tank farms.

SUMMARY

Parametric heat transfer calculations were made for single- and double-shell tanks to predict maximum temperatures possible in the waste and concrete structure during in situ disposal. Transient calculations were carried out until the temperatures of interest reached their peak values with respect to time. Computer runs were made, varying the initial heat generation rate, waste volume, backfill material, and soil overburden. The peak waste and concrete temperatures are plotted as a function of total initial heat loading for the various in situ disposal configurations. Given a tank with a known heat load, the maximum temperature expected under various in situ disposal configurations may be determined. Conversely, given a maximum allowable temperature in the waste or concrete, the maximum heat generation rate may be determined.

For example, if the maximum allowable waste temperature is 350°F, the maximum heat loading in a UGS tank ranges from about 26,000 to 50,000 Btu/hr, depending on tank type and size, waste depth, backfill material, and the presence of overburden material. Similarly, if the temperature in the concrete tank wall is limited to 250°F, then the maximum heat loadings range from about 21,000 to 56,000 Btu/hr.

Further calculations were made to show the dependence of the temperatures on certain input parameters. The thermal conductivity of the waste and soil, the adiabatic boundary radius, and the lower boundary temperature were varied and compared to the "base case" single-shell tank model results. The soil and waste thermal conductivities have the most significant effects on peak temperatures.

9112054051

This analysis does not consider tanks with layered waste. Tanks with most of the heat generating material concentrated on the bottom would have significantly higher temperatures in the waste, base, and wall. Since several tanks fall into this category, it is recommended that individual tanks be analyzed prior to implementation of the in situ disposal option.

RESULTS

GENERAL

The transient heat transfer calculations were made using the HEATING5[3] computer program, using the Classical Implicit Procedure. The detailed geometric models used to represent a single-shell tank and a double-shell tank are shown in Figures 1 and 2, respectively. The locations of temperatures of interest in this report are the peak waste temperature at the tank centerline, the concrete base temperature at the centerline, the peak concrete wall temperature, and the concrete dome temperature at the centerline. The results of the heat transfer analysis are summerized in Table 1, where the peak temperatures in each configuration are correlated to fit the straight line equation given by:

$$Tmax = a \cdot \frac{Po}{1000} + b$$

where:

Tmax is the maximum temperature (^{o}F)

a is the slope of the temperature vs. power curve, $^{o}F/(kBtu/hr)$

Po/1000 is the initial power level converted to kBtu/hr

b is the y-axis intercept at $P_o = 0.0$ (^{o}F).

9 1 1 2 0 5 4 0 5 1 2

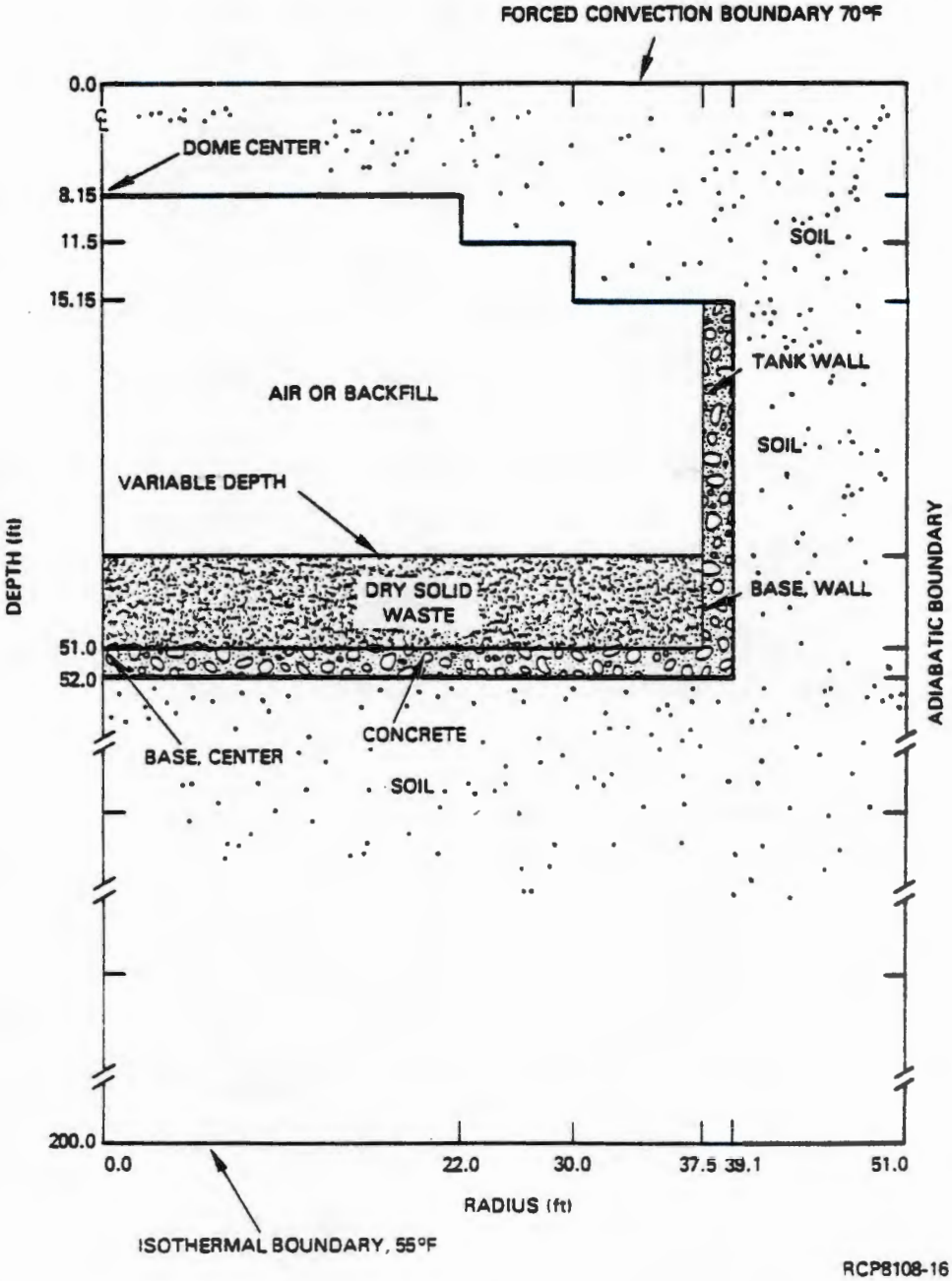

FIGURE 1. Single-Shell Tank Heat Transfer Model.

9112051513

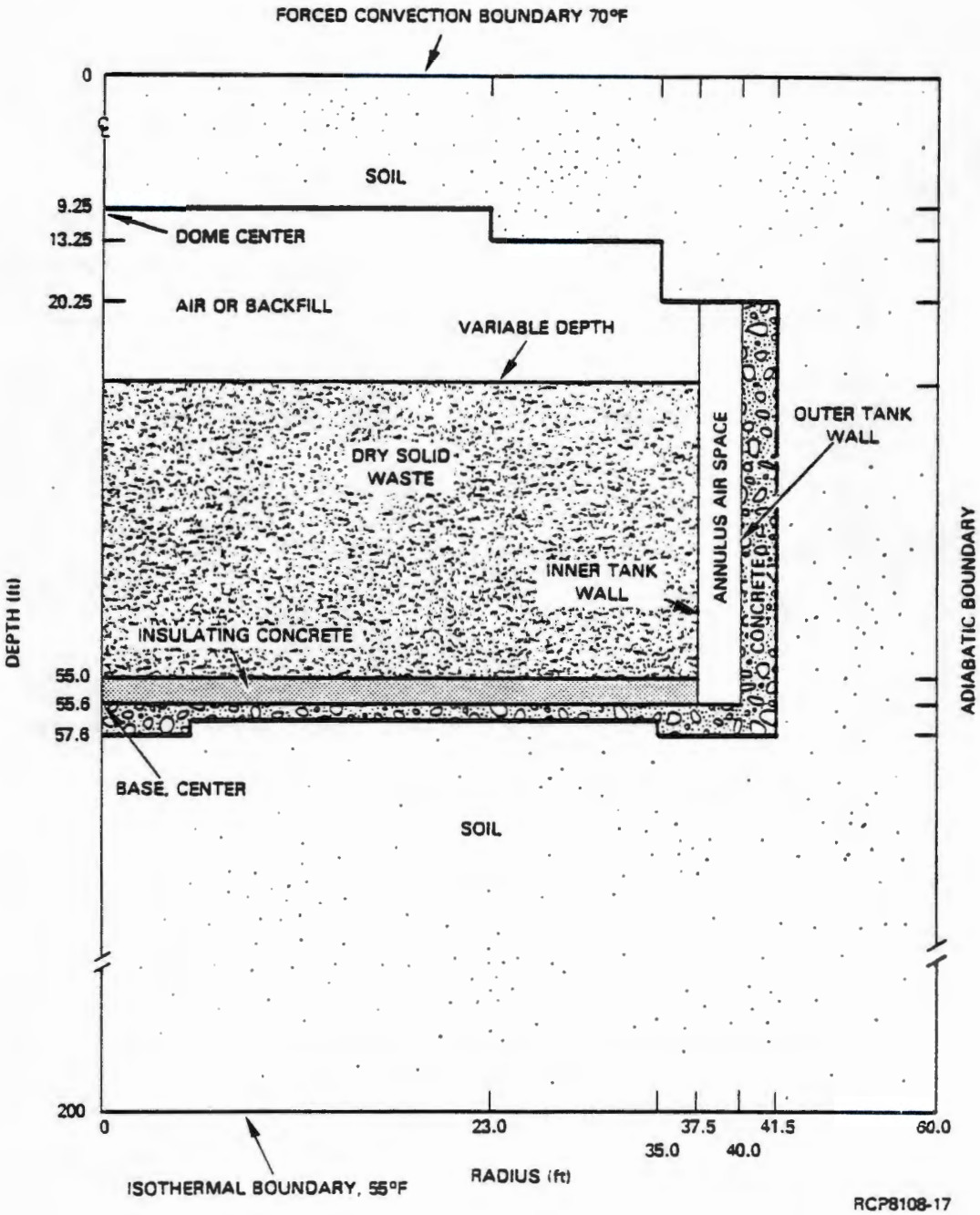

FIGURE 2. Double-Shell Tank Heat Transfer Model.

9 1 1 2 0 5 4 0 5 1 4

TABLE 1. Linear Curve Fit Coefficients.[a]

Tank Type	Backfill Material	Waste Depth (ft)	Peak Waste Temperature		Peak Concrete Temperature					
					Base, Center		Wall		Dome	
			a (^{o}F/kBtu/hr)	b (^{o}F)	a (^{o}F/kBtu/hr)	b (^{o}F)	a (^{o}F/kBtu/hr)	b (^{o}F)	a (^{o}F/kBtu/hr)	b (^{o}F)
Single-Shell (1,000,000 gal)	None	6	5.19	89	5.07	89	3.92	89	4.08	82
		15	5.79	91	5.47	91	4.42	90	3.57	80
		30	6.39	93	5.62	93	4.98	90	2.97	78
	Concrete	6	7.56	92	7.37	92	6.24	90	2.08	76
		15	7.39	92	6.92	92	5.96	89	2.16	76
		30	6.93	94	6.08	92	5.43	90	2.32	78
	Sandy Soil	6	9.31	93	8.9	94	7.34	90	1.46	74
		15	8.72	93	7.93	93	6.79	89	1.61	75
		30	7.44	94	6.44	93	5.77	90	1.97	76
Single-Shell with 13 ft overburden	Sandy Soil	15	9.27	95	8.48	94	7.43	93	3.33	77
Single-Shell (750,000 gal)	None	6	5.4	89	5.26	89	3.86	89	4.26	82
		15	6.03	91	5.64	91	4.44	90	3.7	80
	Concrete	6	7.52	92	7.3	92	5.93	90	2.29	76
		15	7.37	92	6.83	92	5.62	89	2.41	76
	Sandy Soil	6	9.28	93	8.9	94	6.89	90	1.68	74
		15	8.57	93	7.8	93	6.31	89	1.88	75

[a] Used in equation: $T_{max} = a \cdot \frac{P_o}{1000} + b$

TABLE 1. Linear Curve Fit Coefficients (Continued).[a]

Tank Type	Backfill Material	Waste Depth (ft)	Peak Waste Temperature		Peak Concrete Temperature					
					Base, Center		Wall		Dome	
			a (^{o}F/kBtu/hr)	b (^{o}F)	a (^{o}F/kBtu/hr)	b (^{o}F)	a (^{o}F/kBtu/hr)	b (^{o}F)	a (^{o}F/kBtu/hr)	b (^{o}F)
Single-Shell (530,000 gal)	None	6	5.48	89	5.34	89	3.91	89	4.31	82
		15	6.09	91	5.71	91	4.45	90	3.73	80
	Concrete	6	7.22	92	7.06	92	5.52	90	2.59	76
		15	7.04	92	6.56	92	5.18	89	2.74	76
	Sandy Soil	6	8.93	93	8.57	94	6.39	90	1.99	74
		15	7.99	93	7.32	93	5.7	89	2.29	75
Double-Shell	None	6	5.50	91	4.99	93	2.74	98	4.46	84
		15	5.92	94	5.07	95	3.36	95	3.82	83
		30	5.98	98	4.79	99	3.78	94	2.99	81
	Concrete	6	6.93	100	6.42	99	4.51	93	1.70	78
		15	6.87	99	5.97	99	4.40	92	1.80	79
		30	6.39	99	5.10	99	3.93	94	2.02	80
	Sandy Soil	6	8.86	101	7.96	105	5.18	92	1.22	75
		15	8.18	100	6.92	100	4.84	93	1.36	75
		30	7.00	99	5.46	99	4.21	93	1.73	77
Double-Shell with 13 ft overburden	Sandy Soil	15	8.39	102	7.14	101	5.30	94	2.50	81

[a] Used in equation: $T_{max} = a \cdot \frac{P_o}{1000} + b$

The variable "b" would be expected to be between 60° and 70°F, but due to minor nonlinearities in the heat transfer system, higher values resulted. The peak temperature of the waste or concrete may be calculated, if the initial power level or heat load and the other configuration parameters are known. The peak temperatures reported occur 8 to 30 years after time "zero" at disposal, depending on the disposal configuration. This thermal response time is illustrated in Figure 3, where the waste temperatures of four configurations are plotted as a function of time from disposal when the vent system is shut down and the waste is dry and backfill is placed in the tank. The peak temperatures are higher and the time required to reach the peak is longer as heat transfer is further restricted by backfill or overburden. In general, temperatures of the waste, the concrete base center, and the concrete wall increase as waste depth increases with no backfill but decrease as waste depth increases with concrete or sandy soil backfill in the air spaces. However, the concrete dome center temperature decreases as waste depth increases with no backfill and increases with backfill.

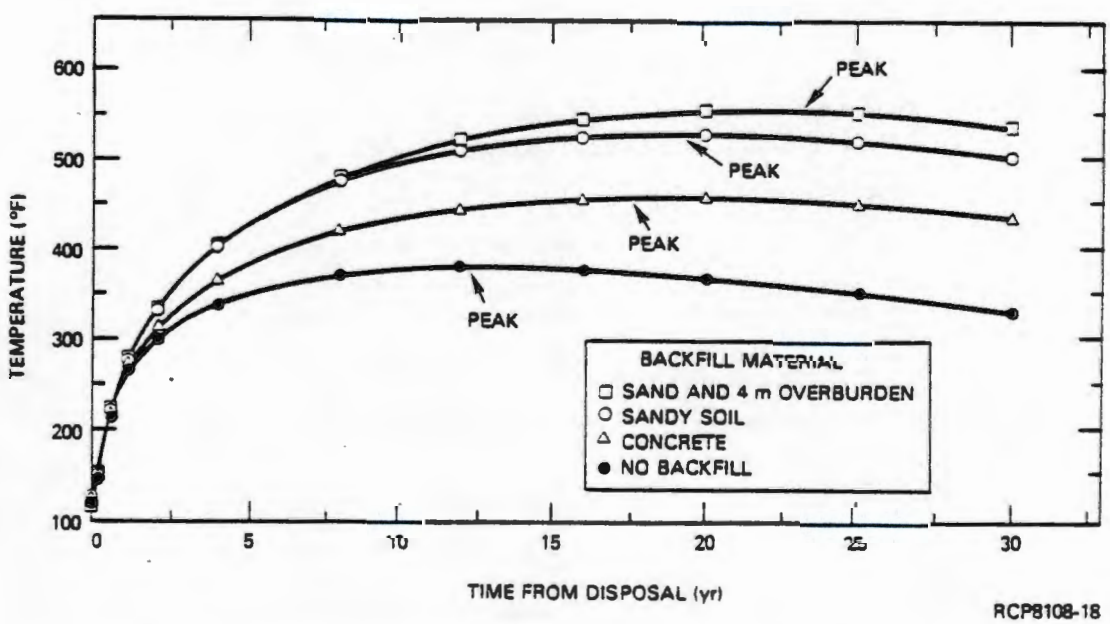

FIGURE 3. Transient Waste Temperatures for a Single-Shell Tank with No Ventilation, a Waste Solids Depth of 15 ft, and Various Backfill Materials in Air Spaces (50,000 Btu/hr).

9112054017

Adding backfill to the air space above the waste and in the annulus in double-shell tanks restricts heat transfer and results in higher temperatures in the waste, concrete base center and concrete wall, but results in lower concrete dome center temperatures. Because the thermal conductivity of the sandy soil is lower than concrete, sandy soil backfill restricts heat transfer more than concrete backfill.

Adding 4 m (13.12 ft) of soil overburden to the existing earth cover resulted in higher temperatures in all locations, because of the increased distance to the upper boundary.

SINGLE-SHELL TANKS

Calculation results for a 1 million gal, single-shell tank are plotted in Figures 4 through 13. Peak waste and concrete temperatures for a tank with no backfill material in the air space and containing dry waste solid depths of 6, 15, and 30 ft are shown in Figures 4, 5, and 6, respectively; the results of adding concrete to the air space for the same three waste depths are shown in Figures 7, 8, and 9, respectively; and the results of substituting sandy soil for concrete as backfill are shown in Figures 10, 11, and 12, respectively.

The results of the calculations for single-shell tanks with 530,000 gal or 750,000 gal nominal capacities are reported in Table 1. Generally, the temperature differences, caused solely by different tank capacities, are less than 10%.

The results of adding 4 m (13.12 ft) of soil overburden to one configuration, that of a 1 million gal, single-shell tank with 15 ft of waste solids and sandy soil backfill, are shown in Figure 13. The largest increase was in the concrete dome temperature while the temperatures in the wall, base, and waste changed little.

DOUBLE-SHELL TANKS

The results for double-shell tanks are plotted in Figures 14 through 23. Peak waste and concrete temperatures for a tank with no backfill and dry waste solid depths of 6, 15, and 30 ft are shown in Figures 14, 15,

9 1 1 2 0 5 4 0 5 1 8

and 16, respectively. The results of adding concrete to the air spaces, including the annulus, are shown in Figures 17, 18, and 19, for the same three waste depths; the results of adding sandy solid backfill are shown in Figures 20, 21 and 22.

The results of placing an additional 4 m (13.12 ft) of soil overburden on top of existing soil on a tank with dry waste solids 15 ft deep and sandy solid backfill are shown in Figure 23. The effect on temperatures is similar to that of the single-shell tank.

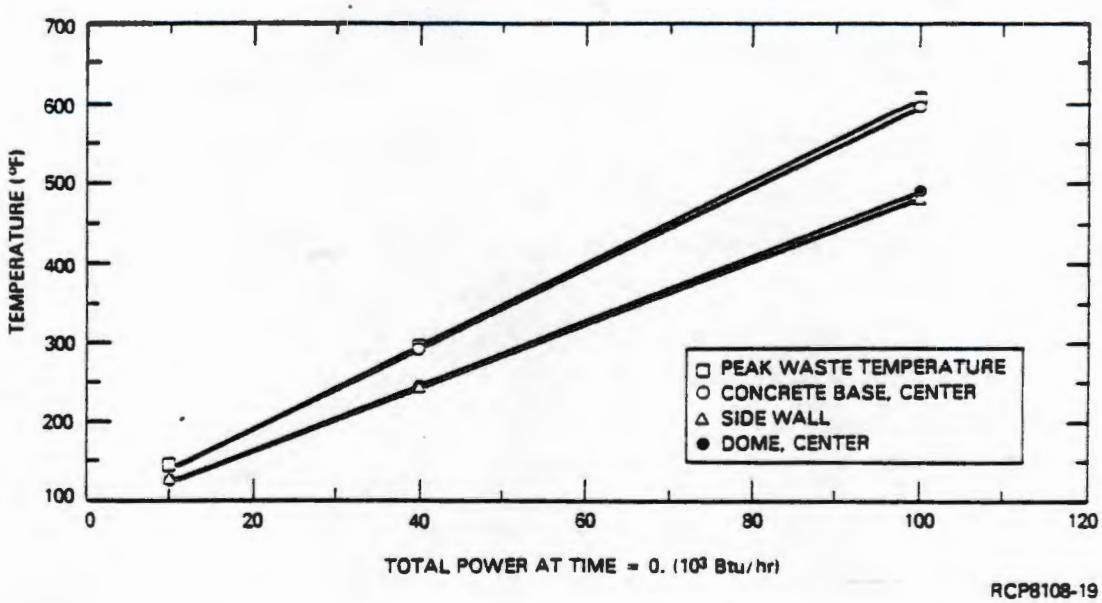

FIGURE 4. Peak Concrete Temperatures for a Single-Shell Tank with No Ventilation, a Waste Solids Depth of 6 ft, and No Backfill Material in Air Spaces.

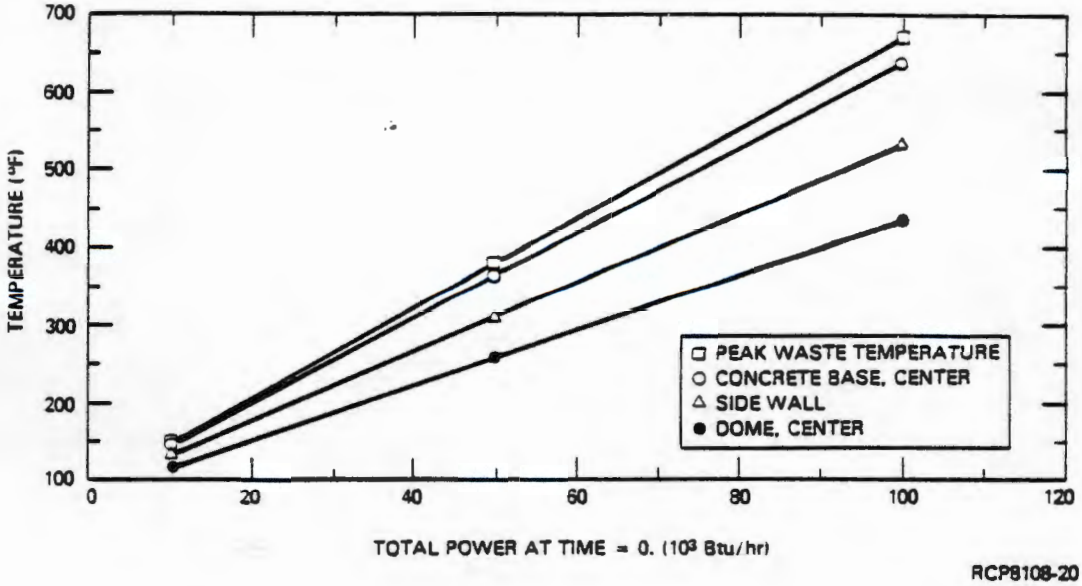

FIGURE 5. Peak Concrete Temperatures of a Single-Shell Tank with No Ventilation, a Waste Solids Depth of 15 ft, and No Backfill Material in Air Space.

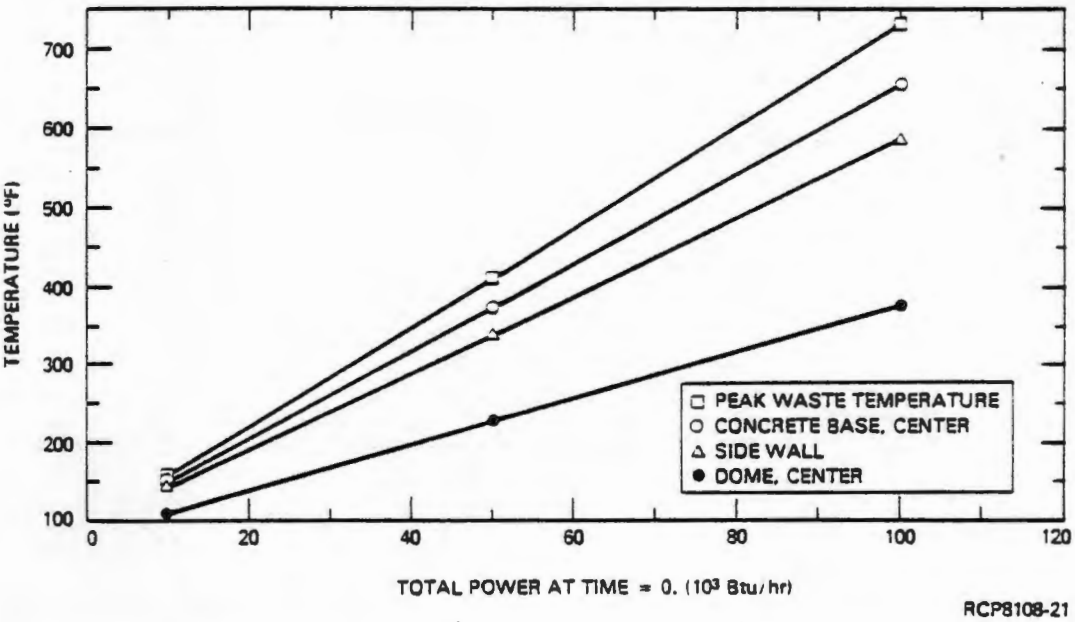

FIGURE 6. Peak Concrete Temperatures of a Single-Shell Tank with No Ventilation, a Waste Solids Depth of 30 ft, and No Backfill Material in Air Spaces.

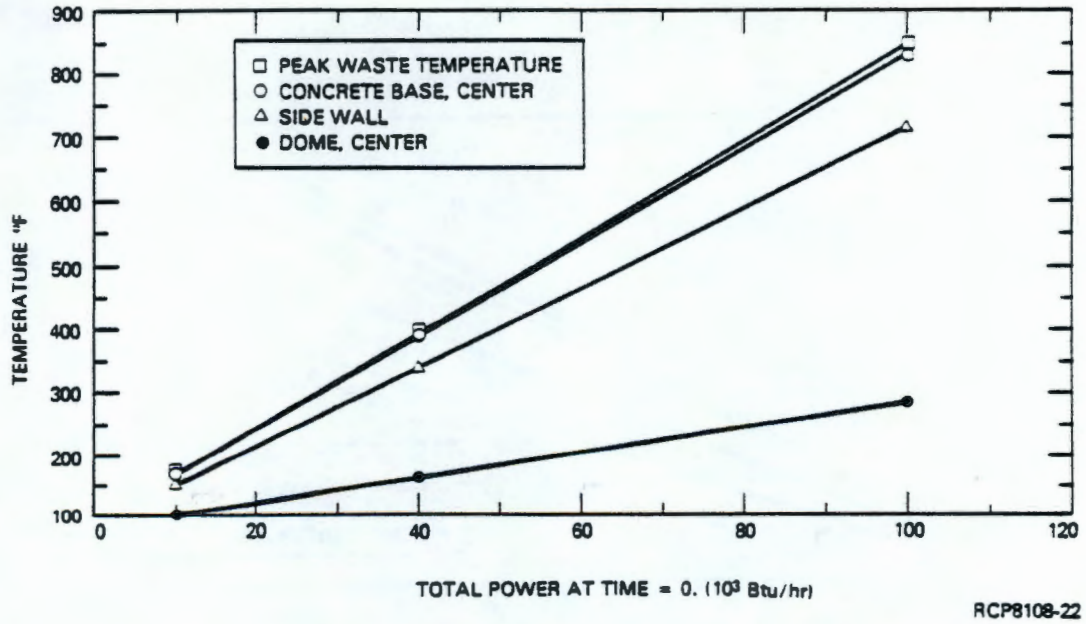

FIGURE 7. Peak Concrete Temperatures of a Single-Shell Tank with No Ventilation, a Waste Solids Depth of 6 ft, and Concrete Backfill in Air Spaces.

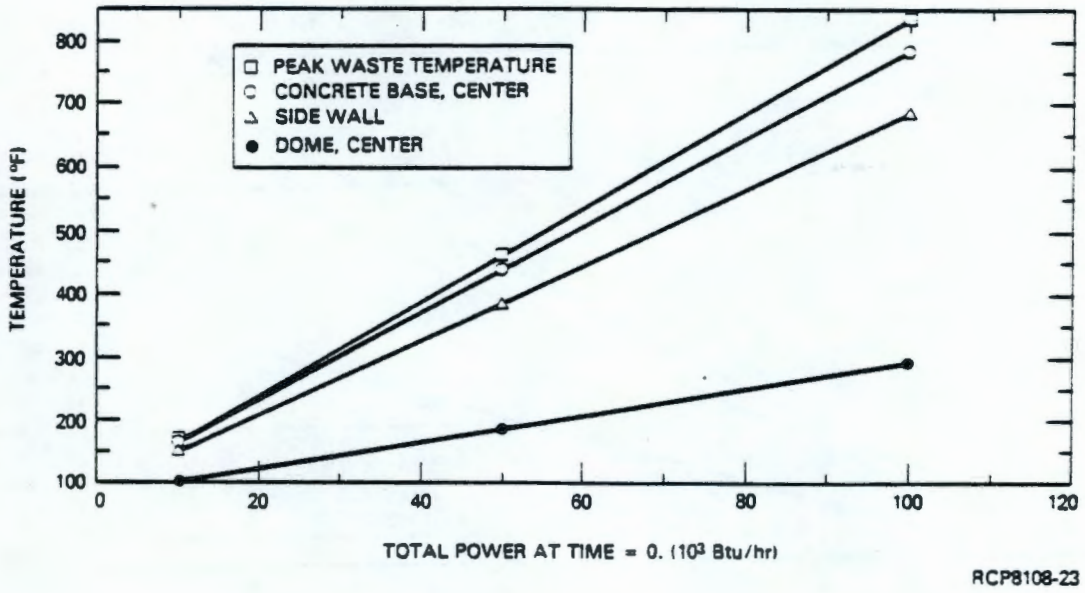

FIGURE 8. Peak Concrete Temperatures of a Single-Shell Tank with No Ventilation, a Waste Solids Depth of 15 ft, and Concrete Backfill in Air Spaces.

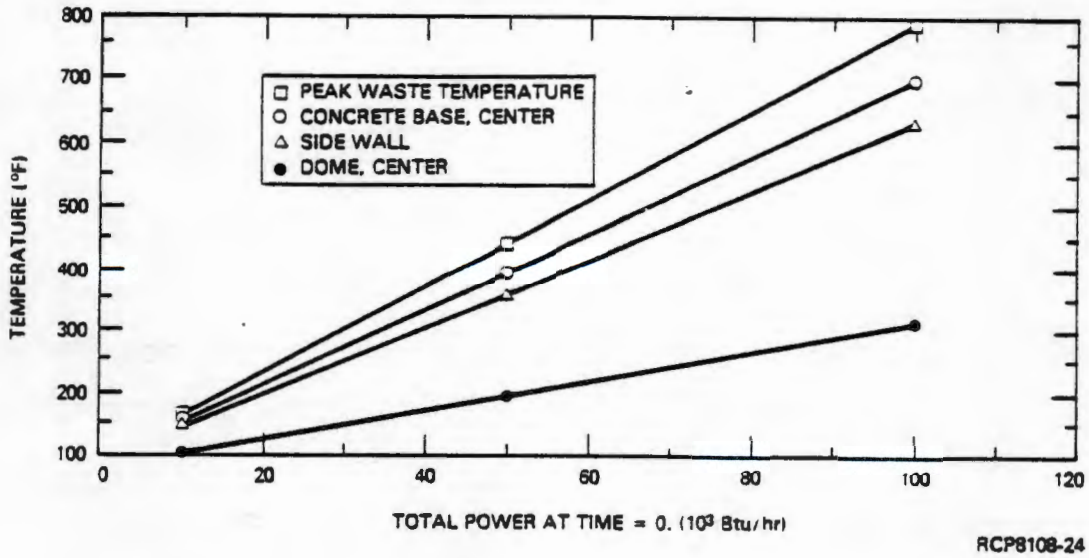

FIGURE 9. Peak Concrete Temperatures of a Single-Shell Tank with No Ventilation, a Waste Solids Depth of 30 ft, and Concrete Backfill in Air Spaces.

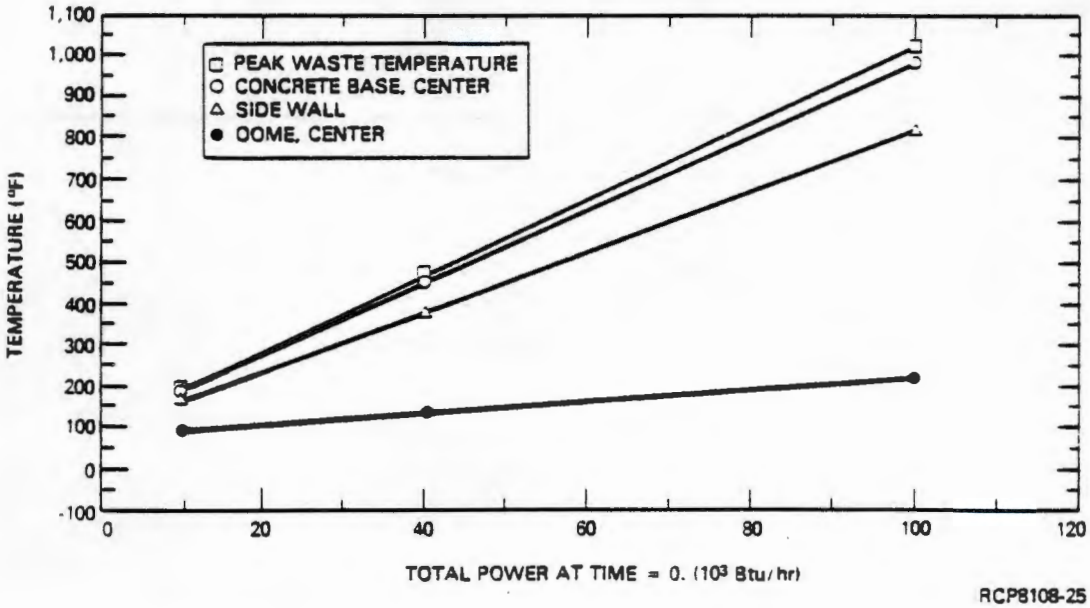

FIGURE 10. Peak Concrete Temperatures of a Single-Shell Tank with No Ventilation, a Waste Solids Depth of 6 ft, and Sandy Soil Backfill in Air Spaces.

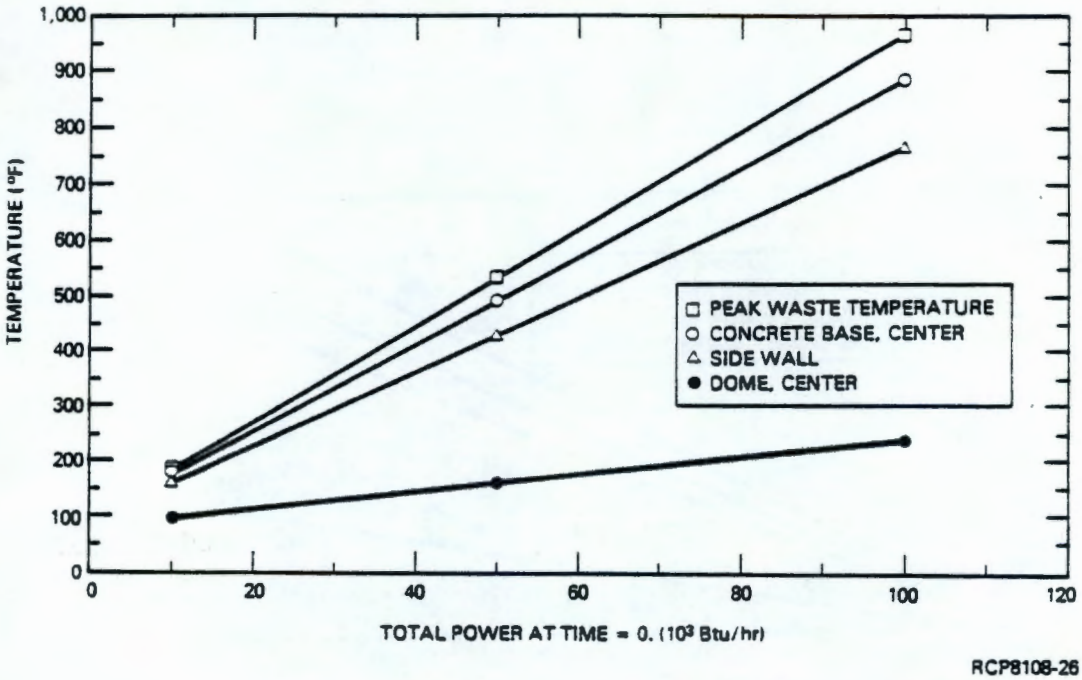

FIGURE 11. Peak Concrete Temperatures of a Single-Shell Tank with No Ventilation, a Waste Solids Depth of 15 ft, and Sandy Soil Backfill in Air Spaces.

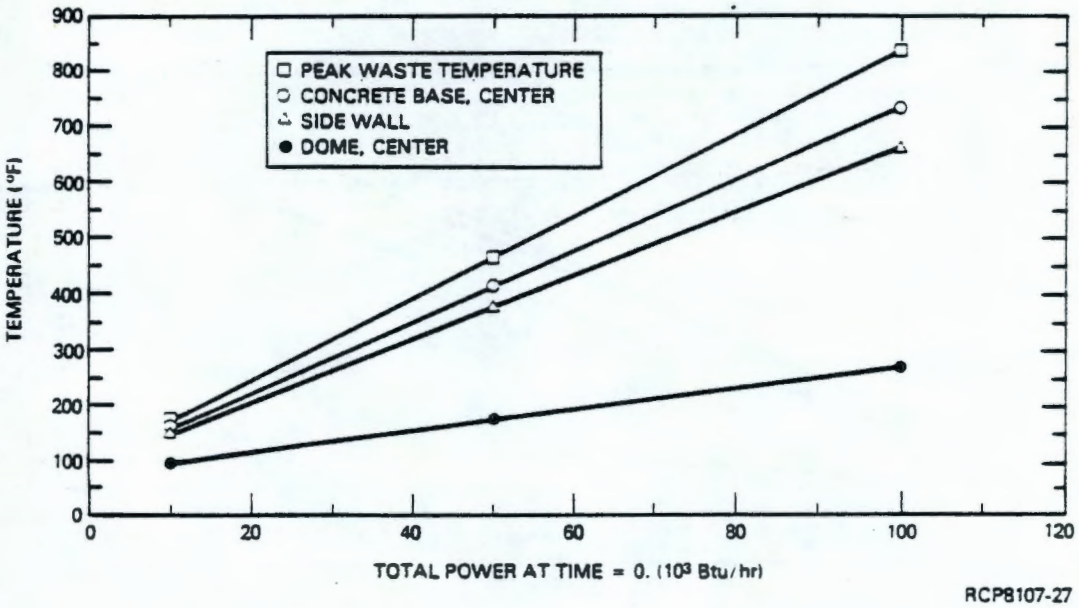

FIGURE 12. Peak Concrete Temperatures of a Single-Shell Tank with No Ventilation, a Waste Solids Depth of 30 ft, and Sandy Soil Backfill in Air Spaces.

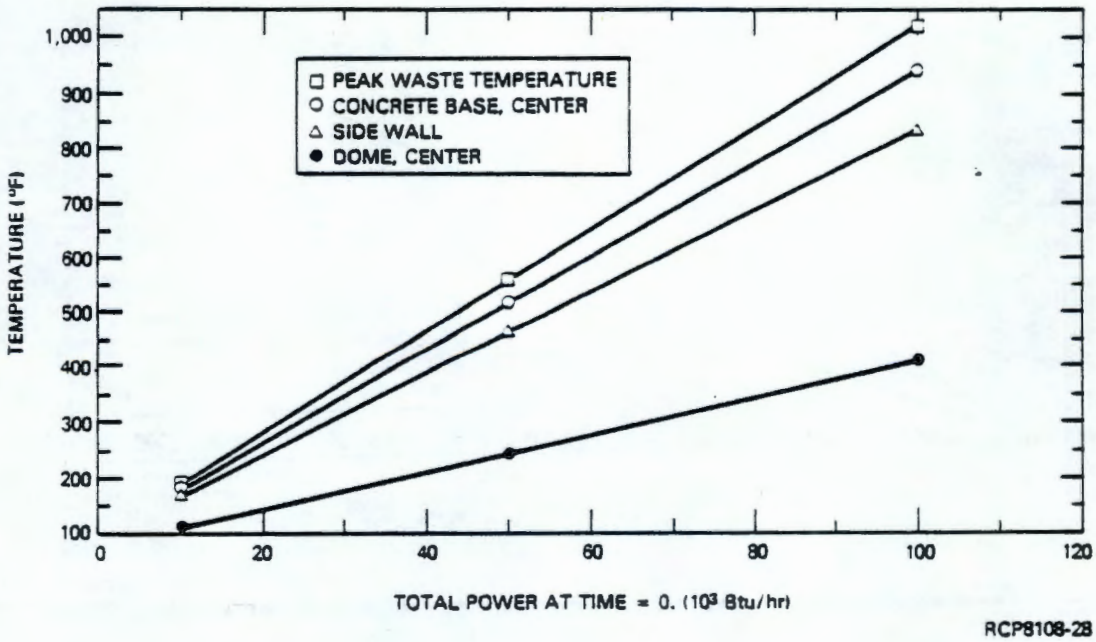

FIGURE 13. Peak Concrete Temperatures of a Single-Shell Tank with 4 m (13.12 ft) of Soil Overburden, a Waste Solids Depth of 15 ft, and Sandy Soil Backfill in Air Spaces.

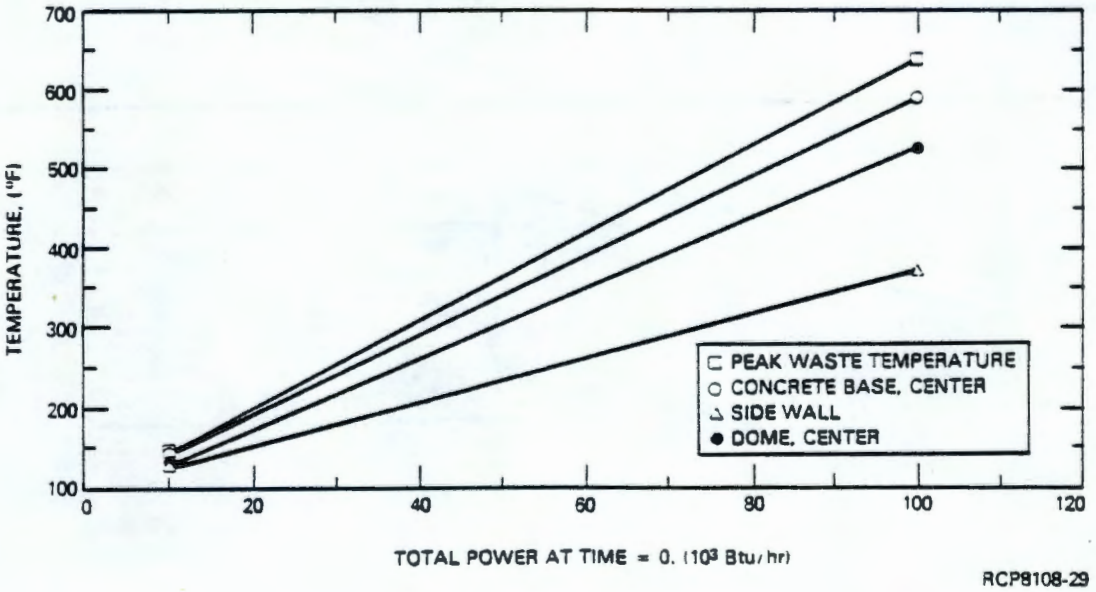

FIGURE 14. Peak Concrete Temperatures of a Double-Shell Tank with No Ventilation, a Waste Solids Depth of 6 ft, and No Backfill Material in Air Spaces.

9112054024

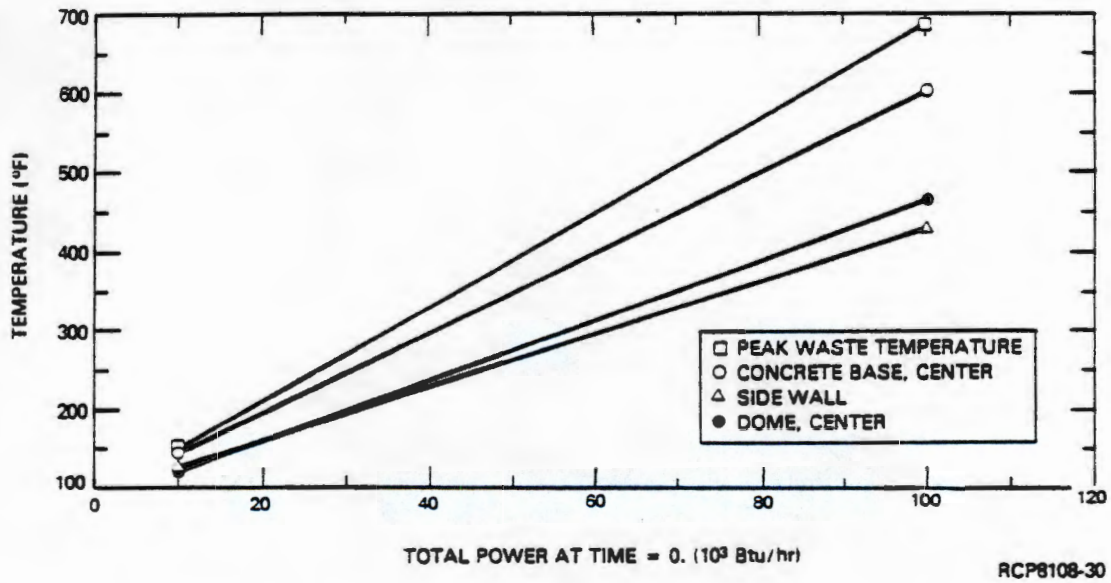

FIGURE 15. Peak Concrete Temperatures of a Double-Shell Tank with No Ventilation, a Waste Solids Depth of 15 ft, and No Backfill Material in Air Spaces.

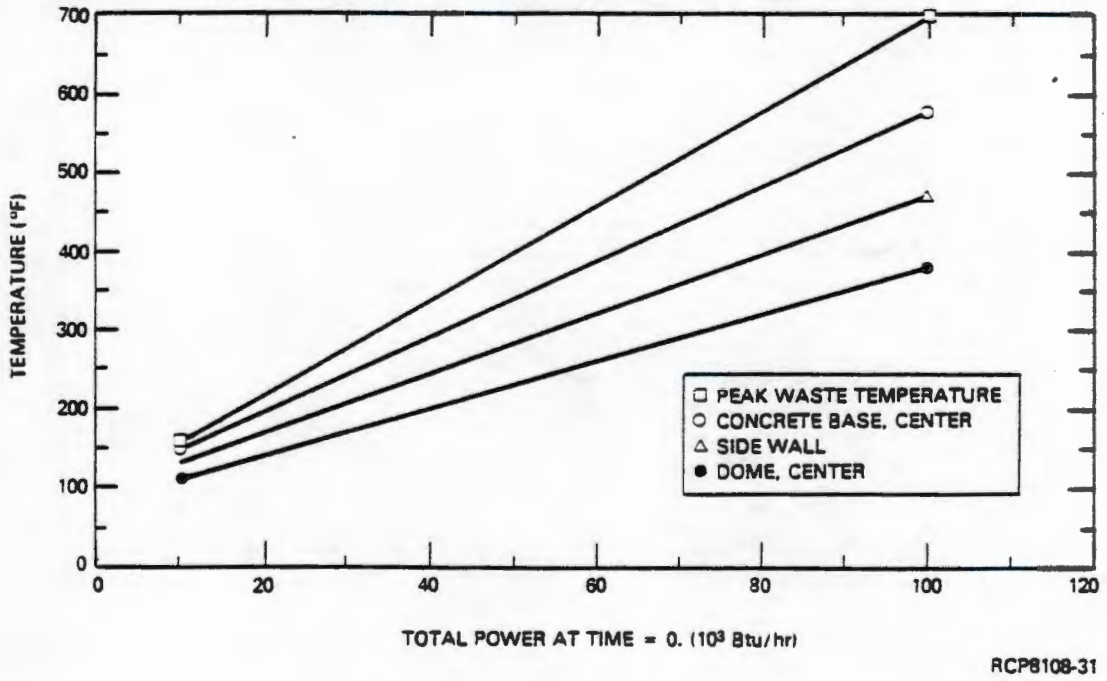

FIGURE 16. Peak Concrete Temperatures of a Double-Shell Tank with No Ventilation, a Waste Solids Depth of 30 ft, and No Backfill Material in Air Spaces.

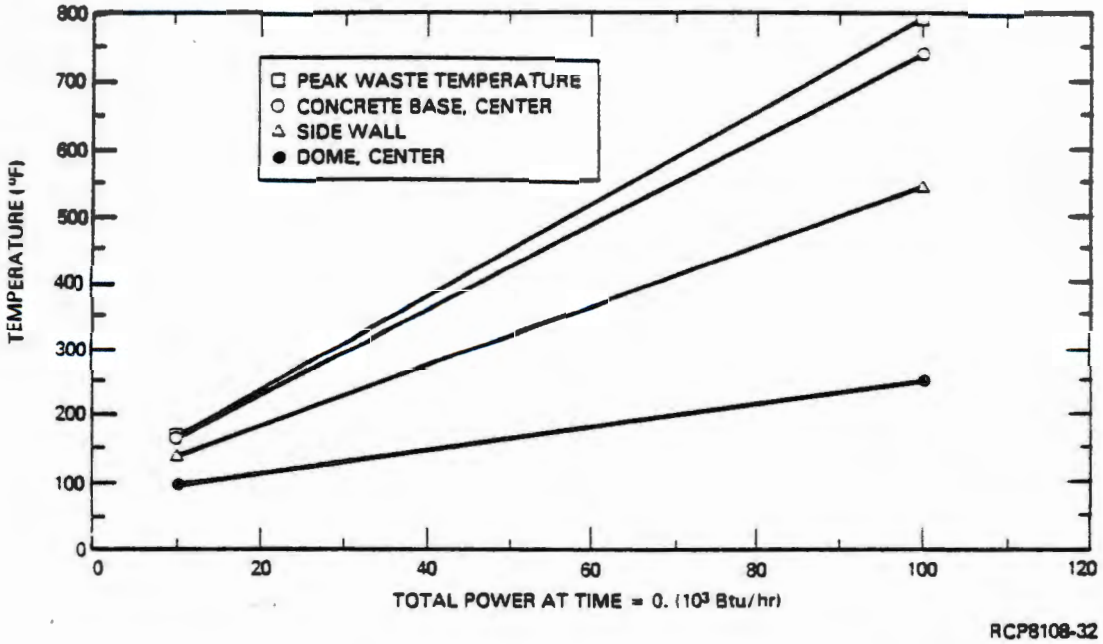

FIGURE 17. Peak Concrete Temperatures of a Double-Shell Tank with No Ventilation, a Waste Solids Depth of 6 ft, and Concrete Backfill in Air Spaces.

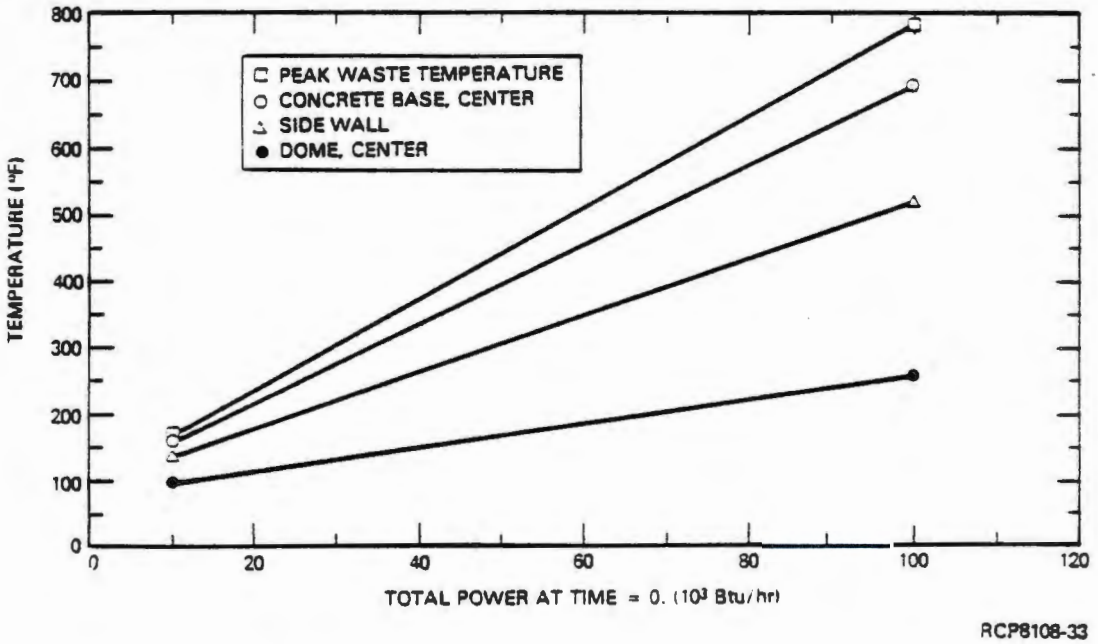

FIGURE 18. Peak Concrete Temperatures of a Double-Shell Tank with No Ventilation, a Waste Solids Depth of 15 ft, and Concrete Backfill in Air Spaces.

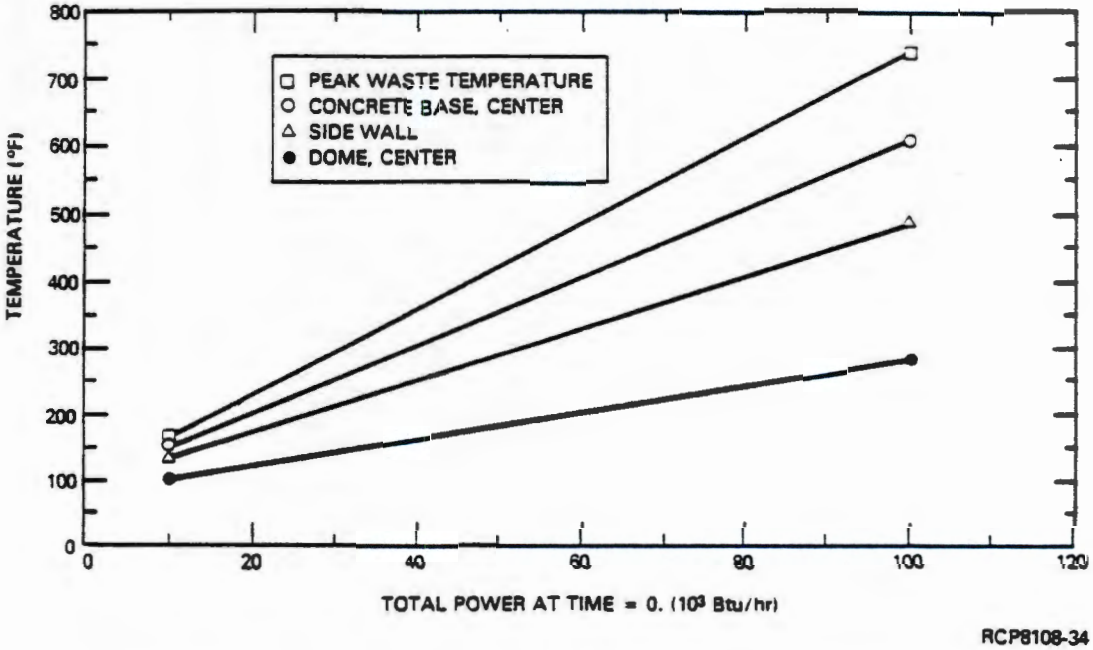

FIGURE 19. Peak Concrete Temperatures of a Double-Shell Tank with No Ventilation, a Waste Solids Depth of 30 ft, and Concrete Backfill in Air Spaces.

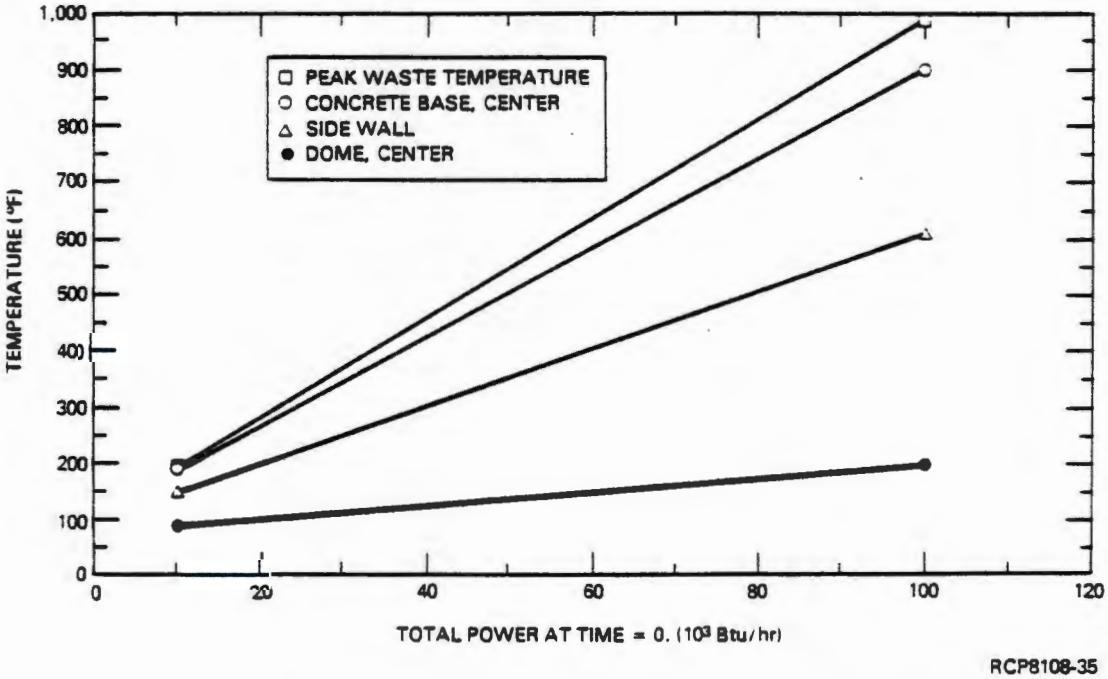

FIGURE 20. Peak Concrete Temperatures of a Double-Shell Tank with No Ventilation, a Waste Solids Depth of 6 ft, and Sandy Soil Backfill in Air Spaces.

9112050527

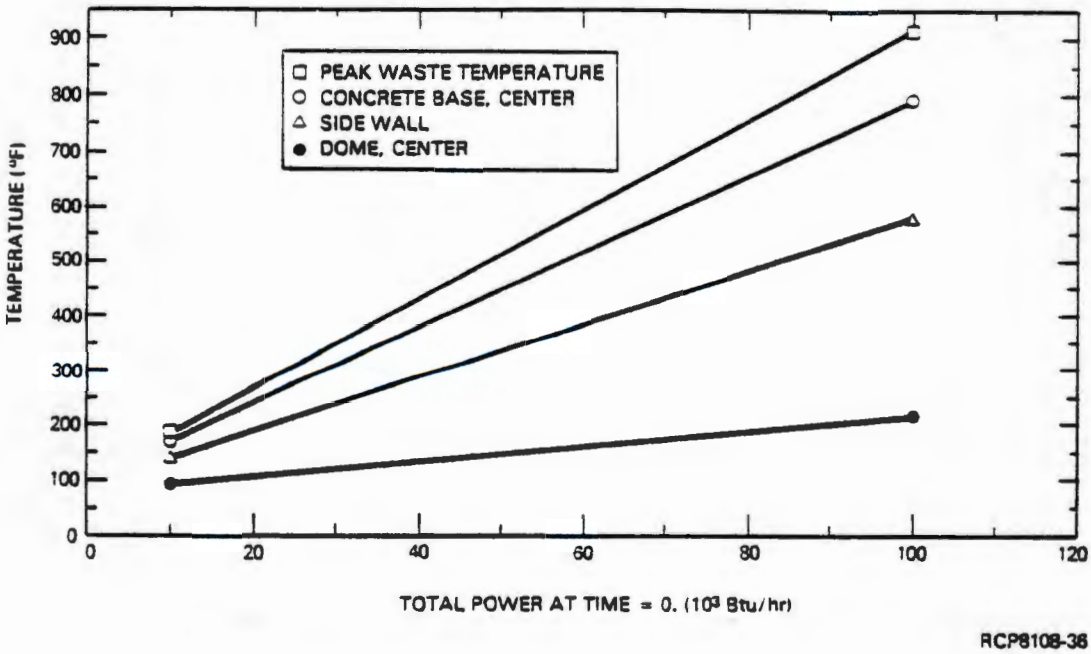

FIGURE 21. Peak Concrete Temperatures of a Double-Shell Tank with No Ventilation, a Waste Solids Depth of 15 ft, and Sandy Soil Backfill in Air Spaces.

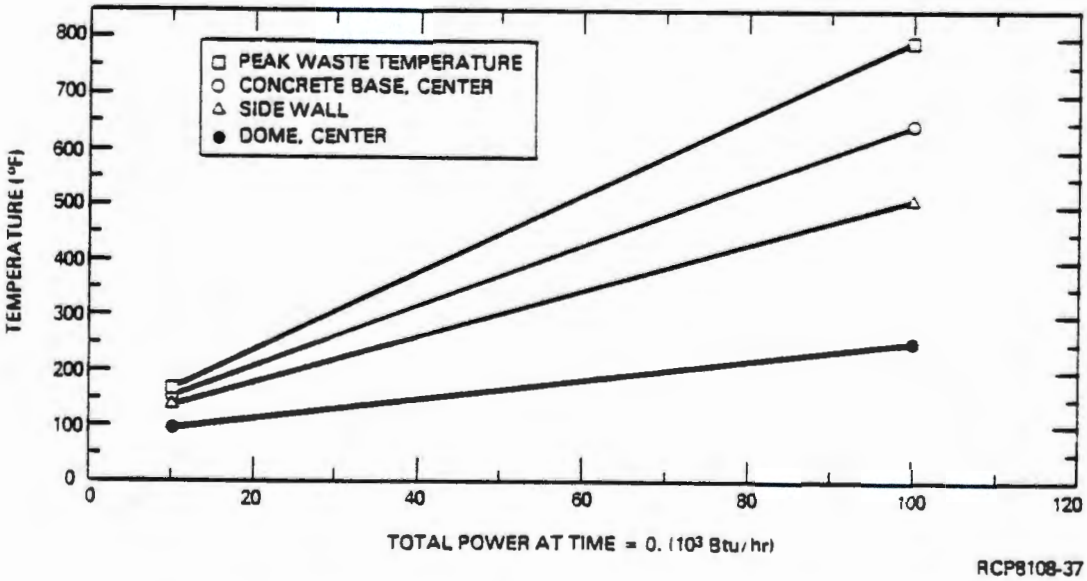

FIGURE 22. Peak Concrete Temperatures of a Double-Shell Tank with No Ventilation, a Waste Solids Depth of 30 ft, and Sandy Soil Backfill in Air Spaces.

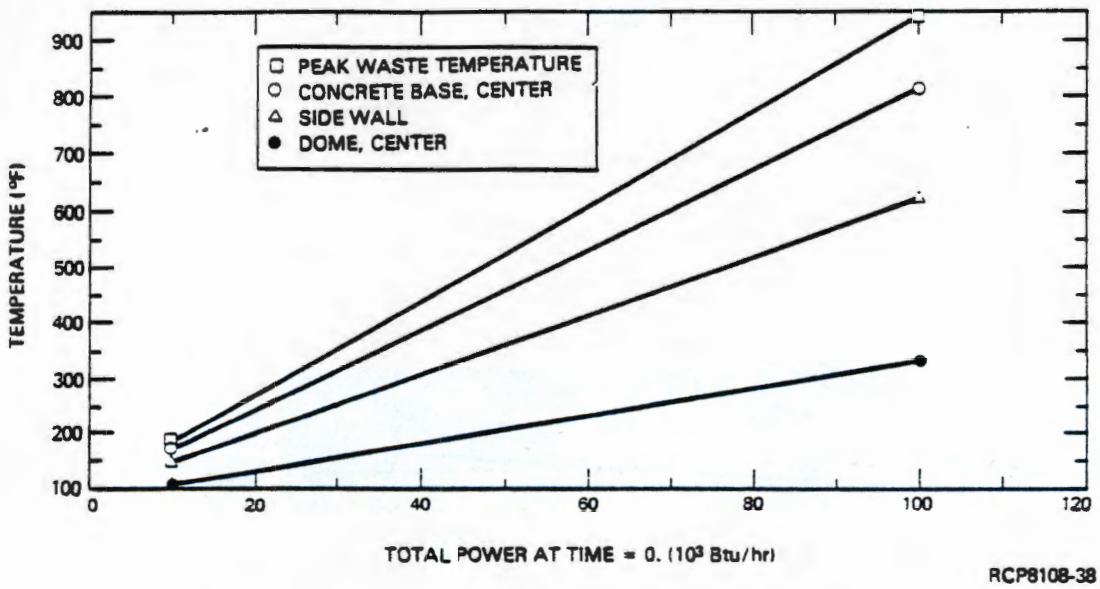

FIGURE 23. Peak Concrete Temperatures of a Double-Shell Tank with 4 m (13.12 ft) Soil Overburden, a Waste Solids Depth of 15 ft, and Sandy Soil Backfill in Air Spaces.

SENSITIVITY ANALYSIS

Due to the variability and uncertainty of the input parameters, calculations were made to show how sensitive the resultant temperatures are to varying certain thermal properties and boundary conditions. The waste thermal conductivity and density, the soil thermal conductivity, the adiabatic boundary radius, and the lower isothermal boundary temperature were each varied, one at a time, to determine their individual effects on peak temperatures. The mathematics of the HEATING5 program was checked on a one-dimensional model and found to be accurate to within $1^{o}F$ (see Appendix B).

The thermal conductivity of the waste solids is dependent on moisture content, density, and the type of waste it is. As a base case, the value of 0.25 Btu/hr·ft·^{o}F was chosen to represent reasonably dry waste and is based on measurements of dry sludge and saltcake samples. The results of varying the waste thermal conductivity from 0.15 to 1.0 Btu/hr·ft·^{o}F for a single-shell tank with waste 15 ft deep,

generating 50,000 Btu/hr, and no backfill, are shown in Figure 24. Increasing the thermal conductivity decreased the temperatures (except for the dome), but had little effect above 0.5 Btu/hr·ft·^{o}F. Increasing the density of the waste from 65 lb/ft^3 to 103 lb/ft^3 decreased all temperatures less than 3%.

The soil thermal conductivity was varied from 0.15 to 0.50 Btu/hr·ft·^{o}F for the single-shell tank model with waste solids 15 ft deep, generating 50,000 Btu/hr, and no backfill. The temperatures as a function of soil thermal conductivity are shown in Figure 25. Soil thermal conductivity has a large effect on the temperatures. Increasing the thermal conductivity through this range caused a 180°F decrease in temperatures. The base case value, 0.25 Btu/hr·ft·^{o}F, is an average value from measurements on Hanford soil.

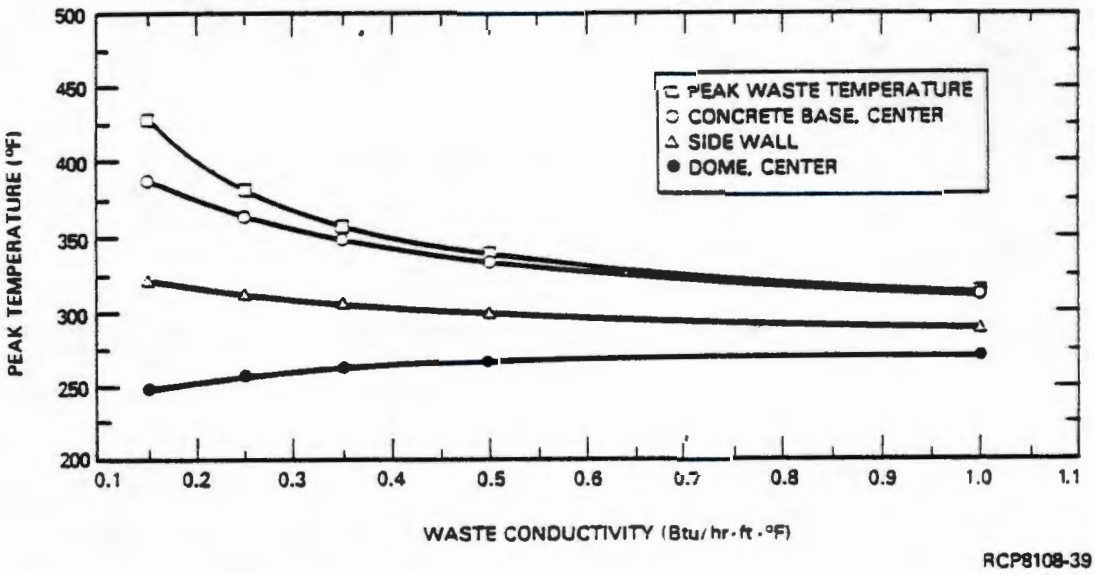

FIGURE 24. Sensitivity to Waste Thermal Conductivity in a Single-Shell Tank with No Ventilation, a Waste Solids Depth of 15 ft, and No Backfill Material in Air Spaces (50,000 Btu/hr).

9112054053 0

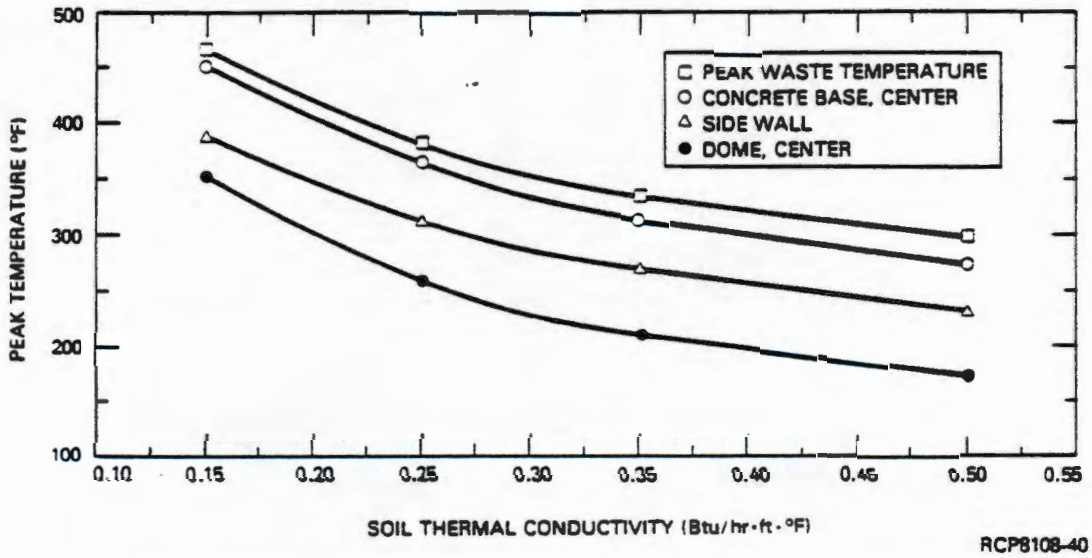

FIGURE 25. Sensitivity to Soil Thermal Conductivity in a Single-Shell Tank with No Ventilation, a Waste Solids Depth of 15 ft, and No Backfill Material in Air Spaces (50,000 Btu/hr).

The 51-ft adiabatic radius for single-shell tanks is derived from half of the 102-ft, center-to-center tank spacing. Due to the cylindrical coordinate system, this boundary is slightly conservative for a tank in the center of 3 x 3 tank array, and is not as good a model for tanks on the side or corner of a tank farm. The adiabatic radius boundary was varied from 51 ft to 80 ft for a 1 million gal single-shell tank with waste 15 ft deep, generating 50,000 Btu/hr, and having no backfill. The results of these calculations are plotted in Figure 26. The peak waste and concrete base temperatures only dropped about 30°F. The concrete wall temperature dropped about 87°F because it is nearer to the boundary; the dome centerline temperature only dropped 11°F. The 60-ft adiabatic boundary, used for the double-shell tank model, is larger than half of the 107-ft, center-to-center spacing because all double-shell tanks are on an edge or corner of a tank farm (no 3 x 3 tank arrays).

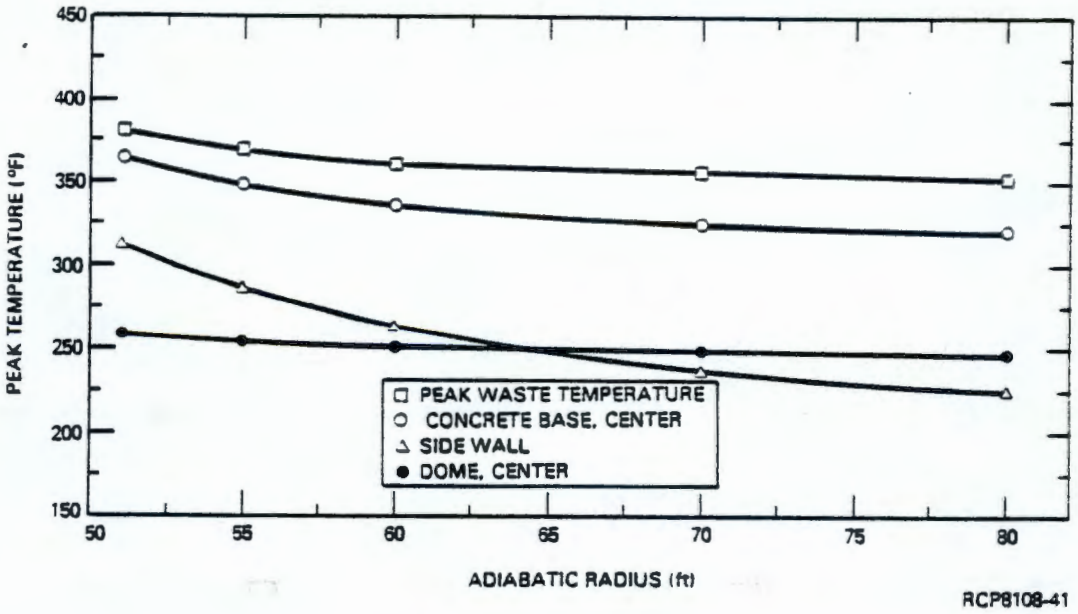

FIGURE 26. Sensitivity to Adiabatic Radius in a Single-Shell Tank with No Ventilation, a Waste Solids Depth of 15 ft, and No Backfill Material in Air Spaces (50,000 Btu/hr).

The isothermal boundary at 200 ft below grade was varied from 55°F to 70°F, resulting in a maximum temperature change of less than 1°F for the four temperatures of interest. This implies that, for practical purposes, an increase or decrease in the average ambient air temperature above the tank would cause an equal change in peak temperatures. However, seasonal fluctations may be neglected, since peak temperatures occurred only after 8 to 30 yrs, depending on the disposal configuration.

THERMAL PARAMETERS AND ASSUMPTIONS

PARAMETERS

The thermal parameters needed to describe heat transfer in UGS tanks are material thermal properties, convection coefficients, boundary conditions, and, in some instances, thermal radiation properties. Heat transfer through waste, structural concrete, soil, and backfill materials is by conduction only. When there is no backfill material, heat transfer

9 1 1 2 0 5 4 0 5 3 2

through the tank vapor space and the annulus in double-shell tanks is by conduction, natural convection, and thermal radiation. The boundaries of the heat transfer model are:

- Forced convection to ambient air at the earth surface
- An isothermal or constant temperature boundary at the 200 ft level below the earth's surface
- An adiabatic or insulated boundary at a constant radial distance from the centerline.

The base case material thermal properties used in these calculations are given in Table 2. The thermal property values are for dry materials and are assumed constant with respect to temperature.

TABLE 2. Thermal Properties.

Material	Thermal Conductivity (Btu/hr·ft·°F)	Density (lb/ft^3)	Specific Heat (Btu/lb·°F)
Air (in air space)	0.016	0.071	0.24
Concrete (including backfill)	0.54	144.0	0.21
Insulating concrete (double-shell tank)	0.11	62.0	0.2
Soil (including backfill)	0.25	113.0	0.22
Waste solids (single-shell tanks)	0.25	65.0	0.3
Waste solids (double-shell tanks)	0.25	103.0	0.3

Radiation interchange factors and natural convection coefficients are listed in Table 3. A radiation interchange factor is the "effective" emissivity, and is a function of emissivity and the shape factor.

9 1 1 2 0 5 4 0 5 3 3

TABLE 3. Interchange Factors and Convection Coefficients.

Location	Radiation Interchange Factor (Dimensionless)	Natural Convection Coefficient ($Btu/hr \cdot ft^2 \cdot {}^oF$)
Vapor Space (6 ft waste)	0.485	$0.22\Delta T^{.33}$
Vapor Space (15 ft waste)	0.529	$0.22\Delta T^{.33}$
Vapor Space (30 ft waste)	0.592	$0.22\Delta T^{.33}$
Double-Shell Tank Annulus	0.674	$0.5\Delta T^{.33}$

The boundary conditions for the top, outer side, and bottom of the heat transfer model are as follows:

- Adiabatic radius for a single-shell tank is 51.0 ft
- Adiabatic radius for a double-shell tank is 60.0 ft
- Isothermal boundary temperature at 200 ft below earth surface is 55^oF
- Ambient air temperature is 70^oF
- Forced convection coefficient at the earth's surface is 2.0 $Btu/hr \cdot ft^2 \cdot {}^oF$.

ASSUMPTIONS

The assumptions needed to model the single- and double-shell tanks for the HEATING5 computer program are included in the following list:

- Axisymmetric symmetry is assumed. The two-dimensional cylindrical (R, Z coordinates) heat transfer models are defined in Figures 1 and 2. This assumption tends to make the calculations conservative by reducing the surface area through which heat is transferred to the upper and lower boundaries.
- The waste material is assumed to be a cylindrical slab of uniform thickness, thermal conductivity, and power density. Actual tanks have layered solids and varying degrees of nonuniformity

9 1 1 2 0 5 4 0 5 3 4

of thermal properties. The resultant temperatures may be somewhat higher or lower, depending on how the heat-generating material is distributed.

- A decay rate half-life of 30 yr is assumed because most of the heat generated is by strontium or cesium decay. This enters into the calcultions, because the peak temperatures reported in Figures 4 through 23 occur from 8 to 30 yr after "zero" time at disposal.
- All air ventilation cooling systems are assumed to be off. Currently, tanks with enough heat generation to be considered a problem are on ventilating systems.
- The concrete in the tank dome of both models is assumed to have the same thermal properties as soil so that the dome curvature could be modeled. Making this conservative and simplifying assumption results in a very slight temperature increase.

9112054053 5

REFERENCES

1. U. S. Energy Research and Development Administration, Alternatives for Long-Term Management of Defense High-Level Radioactive Waste, ERDA-77-44, Hanford Site, Richland, Washington (September 1977).

2. Rockwell Hanford Operations, Technical Aspects of Long-Term Management Alternatives for High-Level Defense Waste at the Hanford Site, RHO-LD-141, Rockwell Hanford Operations, Richland, Washington (October 1980).

3. W. D. Turner, D. C. Elrod, and I. I. Siman-Tov, HEATING5 - An IBM 360 Heat Conduction Program, ORNL/CSD/TM-15, Oak Ridge National Laboratory, Oak Ridge, Tennessee (March 1977).

4. W. L. McCabe, and J. C. Smith, Unit Operations of Chemical Engineering, Second Edition, pp 395-405, McGraw-Hill Company, New York (1967).

9 1 1 2 0 5 4 0 5 3 6

THIS PAGE
INTENTIONALLY
LEFT BLANK

RHO-LD-171

APPENDICES

9 1 1 2 0 5 4 0 5 3 7

THIS PAGE
INTENTIONALLY
LEFT BLANK

APPENDIX A

SURVEY OF HANFORD TANK HEAT LOADS

A review of readily available data records was made to estimate bulk heat loading in Hanford waste tanks. Since heat generation rates cannot be measured directly, psychrometric data from tank ventilation systems and some solid waste sample analytical data were analyzed to obtain the list of single-shell tanks and estimated heat loads in Table A-1. Psychrometric readings are generally more reliable than solid waste analytical data (due to the number of readings), so most of the estimates listed come from psychrometric data input plus an estimated heat loss by conduction.

This table gives an indication of how many single-shell tanks have more than 20,000 Btu/hr and gives an estimate of their respective heat loads. Psychrometric data is being taken monthly on most of the tanks listed. Heat generation rate estimates may vary from one report to the next because more data is available as time goes on and because of the inherent problems in making this kind of estimate.

Based on results of chemical analysis of double-shell slurry feed and product supernatant samples, the heat generation rate of wastes to be stored in double-shell tanks ranges typically from 40,000 to 90,000 Btu/hr per million gallons of concentrated liquor. When these liquid wastes are solidified (as in preparation for in situ disposal), the heat generation rate would be higher by a factor of 1.2 to 2.0 depending on the method used for drying and solidifying the waste.

9 1 1 2 0 5 4 0 5 3 8

TABLE A-1. Hanford Tank Heat Loadings.

Tank	Average Waste Depth (ft)	Estimated Heat Generation Rate (Btu/hr)
101-A	28.2	20,000 ± 10,000*
104-A	0.85	60,000 ± 40,000*
105-A	0.57	60,000 ± 40,000
106-A	2.84	40,000 ± 20,000*
103-AX	3.60	20,000 ± 10,000*
104-AX	0.09	20,000 ± 10,000*
104-BY	18.8	20,000 ± 10,000
105-BY	18.9	30,000 ± 15,000
106-BY	18.9	20,000 ± 10,000
103-C	5.30	20,000 ± 10,000*
105-C	4.54	40,000 ± 20,000
106-C	5.96	180,000 ± 40,000
107-C	10.2	20,000 ± 10,000*
101-S	12.6	25,000 ± 10,000
102-S	16.8	20,000 ± 10,000
103-S	6.99	20,000 ± 10,000
107-S	10.3	15,000 ± 10,000
110-S	20.9	15,000 ± 10,000
101-SX	13.8	30,000 ± 20,000*
102-SX	15.7	30,000 ± 20,000*
103-SX	19.2	30,000 ± 20,000*
104-SX	21.6	30,000 ± 20,000*
105-SX	20.4	30,000 ± 20,000*
107-SX	3.30	45,000 ± 20,000
108-SX	2.63	54,000 ± 20,000
109-SX	7.78	60,000 ± 30,000
110-SX	1.18	50,000 ± 20,000
111-SX	3.78	53,000 ± 20,000
112-SX	3.21	50,000 ± 25,000
114-SX	6.05	70,000 ± 35,000

*No Psychrometric data available.

9 1 1 2 0 5 4 0 5 3 9

APPENDIX B

HEATING5 CODE CHECK CALCULATIONS

A one-dimensional heat conduction problem was selected to compare the HEATING5 calculational method to the results of an exact solution. The problem of the uniformly heated, semi-infinite slab was modeled for HEATING5. The slab is 30 ft thick and generates heat according to the equation:

$$Q = Q_o e^{-\lambda t} \text{ for } t \geq 0.$$

where:

Q_o is the Initial Power Density (Btu/hr ft^3)

$-\lambda$ is $\ln(0.5)/\tau$; τ = half-life = 30 yr = 2.63E+5 hr

$-\lambda$ is -2.636E-6 hr^{-1}

t is time (hr).

The two surfaces are held constant at 0.0°F and the initial slab temperature is 0.0°F. The transient temperatures were calculated over a 10 yr (87,660 hr) period. Selected results of the HEATING5 calculations are compared in Table B-1 with the results of the exact solution given by the following equation:(1)

$$T = \frac{\kappa Q_o}{\lambda k}\left(\frac{\cos(x\sqrt{\lambda/\kappa})}{\cos(\ell\sqrt{\lambda/\kappa})} - 1\right) e^{-\lambda t} + \frac{4\kappa Q_o}{\pi\lambda k}\sum_{n=o}^{\infty}\frac{(-1)^n\, e^{-\kappa(2n+1)^2\pi^2 t/4\ell^2}}{(2n+1)}\frac{\cos((2n+1)\pi x/2\ell)}{(1-((2n+1)^2\pi^2\kappa/(4\lambda\ell^2)))}$$

where:

T is the temperature at point x and time t

κ is the thermal diffusivity (ft^2/hr)

k is the thermal conductivity ($Btu/hr \cdot ft \cdot {}^oF$)

x is the distance from slab center (ft)

ℓ is 15 ft, $-\ell \leq x \leq \ell$

e is 2.71828...

π is 3.14159...

The summation on the right side of the equation converges within 40 terms for small values of t and within 4 terms for large values of t. The results in Table B-1 show that the finite differencing method in HEATING5 is accurate to within 1^oF in the test problem.

TABLE B-1. Temperatures at Point x and Time t for HEATING5 and Exact Solution.

t, time (hr)	x, Distance from center of slab (ft)					
	0.0		6.0		12.0	
	HEATING5	EXACT	HEATING5	EXACT	HEATING5	EXACT
1.0	0.08	0.08	0.08	0.08	0.08	0.08
10.0	0.77	0.77	0.77	0.77	0.76	0.77
100.0	7.69	7.69	7.69	7.69	6.97	7.36
1,000.0	76.04	76.34	72.24	72.84	43.08	43.6
8,766.0 (1 year)	370.40	371.39	313.31	314.11	136.91	137.21
35,064.0 (4 years)	415.37	415.32	348.77	348.74	149.30	149.28
87,660.0 (10 years)	361.83	361.81	303.81	303.79	130.05	130.04

REFERENCE

1. H. S. Carslaw, and J. C. Jaeger, Conduction of Heat in Solids, second edition, p 132, Oxford Press, Cambridge (1959).

9 1 1 2 0 5 4 0 5 4 1

DISTRIBUTION

Number of Copies	
OFFSITE	
3	Argonne National Laboratory J. H. Kittel (2) M. J. Steindler
1	Colorado State University F. W. Whicker
1	Cornell University J. C. Smith
2	U.S. Department of Energy Albuquerque Operations Office R. Y. Lowrey (2)
1	U.S. Department of Energy Chicago Operations Office S. A. Mann
6	U.S. Department of Energy Headquarters G. A. Daly J. E. Dieckhoner C. A. Heath D. J. McGoff G. K. Oertel R. D. Walton, Jr.
1	U.S. Department of Energy Idaho Falls Operations Office J. P. Hamric
2	U.S. Department of Energy Oak Ridge Operations Office S. W. Ahrends (2)
2	U.S. Department of Energy San Francisco Operations Office S. G. Harbinson (2)

9112054054 2

3 U.S. Department of Energy
Savannah River Operations Office

E. S. Goldberg
T. B. Hindman, Jr.
W. B. Wilson

7 U.S. Department of Energy
E. I. du Pont de Nemours and Company
Savannah River Laboratory

W. R. Cornman
J. L. Crandall
R. G. Garvin
D. E. Gordon
P. L. Gray
D. L. McIntosh
J. A. Stone

1 U.S. Department of Energy
Savannah River Plant

R. Maher

1 Exxon Nuclear Idaho

G. L. Ritter

1 Lawrence Livermore Laboratory

J. D. Tewhey

1 North Carolina State University

H. Palmer, III

2 Oak Ridge National Laboratory

T. H. Row
R. E. Blanco

1 Office of Nuclear Waste Isolation
Battelle Memorial Institute - Columbus

W. Carbeiner

1 Pennsylvania State University

R. Roy

9 1 1 2 0 5 4 0 5 4 3

3	Rockwell International Canoga Park, California Energy Systems Group J. Burton L. Maki A. B. Martin (2)
1	Sandia Laboratories Albuquerque, New Mexico R. G. Kepler
1	Stanford University I. Remson
1	University of Florida L. L. Hench
1	Vanderbilt University F. L. Parker
1	27071-B Calle Caballero San Juan Capistrano, California D. C. Van Dine

ONSITE

4	U.S. Department of Energy Richland Operations Office E. A. Brachen J. J. Schreiber M. W. Shupe F. R. Standerfer
2	Hanford Engineering Development Laboratory A. G. Blasewitz R. E. Lerch

9 1 1 2 0 5 4 0 5 4 4

ONSITE

10 Pacific Northwest Laboratory

W. F. Bonner
T. D. Chikalla
L. T. Lakey
D. E. Larson
J. L. McElroy
R. D. Nelson
A. M. Platt
J. V. Robinson
W. A. Ross
C. M. Unruh
L. D. Williams

65 Rockwell Hanford Operations

B. N. Anderson
D. C. Bartholomew
S. S. Bath
G. A. Beitel
D. E. Braden
G. D. Campbell (10)
C. DeFigh-Price
J. L. Deichman
R. A. Deju
L. E. Edvalson
G. D. Forehand
S. A. Gallagher
K. A. Gasper
J. F. Geiger
D. G. Harlow
M. K. Harmon
B. A. Higley
K. M. Hodgson
H. H. Hopkins, Jr.
F. M. Jungfleisch
R. G. Johnston
J. D. Kaser
R. L. Koontz
M. J. Kupfer
H. E. McGuire
L. P. McRae
D. L. Merrick
J. H. O'Brien
R. G. Oliver

9 1 1 2 0 5 4 0 5 4 5

ONSITE

Rockwell Hanford Operations (Continued)
R. A. Palmer
K. J. Pascoe
I. E. Reep
R. C. Roal
J. H. Roecker
W. W. Schulz
P. F. Shaw
J. P. Slaughter
M. J. Smith
C. R. Stroup
R. J. Thompson
D. L. Uebelacker
D. L. Uhl
J. L. Walker
R. A. Watrous
J. R. Wetch
S. A. Wiegman
D. D. Wodrich
D. E. Wood
J. R. Wright
Document Control (4)
RCP (3)

9 1 1 2 0 5 4 0 5 4 6

THIS PAGE
INTENTIONALLY
LEFT BLANK